**Influence of inter-domain dynamics and surrounding environment flexibility on the direct electrochemistry and electrocatalysis of self-sufficient cytochrome P450 3A4-BMR chimeras**

Influence of inter-domain dynamics and surrounding environment flexibility on the direct electrochemistry and electrocatalysis of self-sufficient cytochrome P450 3A4-BMR chimeras

By: Castrignano, Silvia; Di Nardo, Giovanna; Sadeghi, Sheila J.; et al.

JOURNAL OF INORGANIC BIOCHEMISTRY Volume: 188 Special Issue: SI Pages: 9-17 doi 10.1016/j.jinorgbio.2018.08.003

# Influence of inter-domain dynamics and surrounding environment flexibility on the direct electrochemistry and electrocatalysis of self-sufficient cytochrome P450 3A4-BMR chimeras

Silvia Castrignanò, Giovanna Di Nardo, Sheila J. Sadeghi, Gianfranco Gilardi*

Department of Life Sciences and Systems Biology, University of Torino, Via Accademia Albertina 13, Torino, Italy.

*Corresponding author.

Email address: gianfranco.gilardi@unito.it

Fax: +39-011-6704643.

Tel.: +39-011-6704593.

**Abstract**

The linker region of multi-domain enzymes has a very important role for the interconnection of different enzyme modules and for the efficiency of catalytic activity. This is particularly evident for artificial chimeric systems. We characterised an artificial self-sufficient enzyme developed by genetic fusion of the catalytic domain of cytochrome P450 3A4 and reductase domain of *Bacillus megaterium* BM3 (BMR).

Here we report the direct electrochemistry of 3A4-BMR chimeras immobilised on glassy carbon electrodes and we investigated the effect of inter-domain loop length and immobilising environment flexibility on both redox properties and electrocatalysis. We observe that redox potential can be modulated by the linker length and the immobilising layer flexibility. In addition, enzyme inter-domain dynamics and environment flexibility also modulate 3A4-BMR turnover efficiency on electrode system. $V_{max}$ values are increased up to about 100 % in the presence of testosterone and up to about 50 % in presence of tamoxifen by decreasing immobilising film rigidity. The effect on 3A4-BMR $V_{max}$ values is dependent on inter-domain loop length with 3A4-5GLY-BMR chimera being the more affected. The underlying reason for these observations is the potential motion of the FMN domain that is the key to shuttle electrons from FAD to heme.

**Keywords:**

P450 3A4-BMR; Glycine linker; Electron transfer; Electrocatalysis.

## 1. Introduction

Protein engineering aimed to the development of self-sufficient multi-domain enzymes is an important approach for the development of enzymatic systems suitable for biotechnological research. The very well established importance of P450 enzymes in drug catalysis, pharmacokinetics and pharmacogenomics is the rationale for the development of efficient bio-analytical platforms that could mimic these complex enzyme systems especially concerning electron transfer pathway with redox partners, coupling efficiency and catalytic activity [1-5]. Our laboratory has developed a chimeric enzyme system involving human P450 3A4 catalytic domain and the reductase domain of *B. megaterium* P450 BM3 (BMR) connected using glycine peptide loops of different length that proved to be more stable than the native P450 3A4 enzyme [6-8]. We demonstrated that, in agreement with what previously established for multi-domain enzyme systems [9], the inter-domain mutual connectivity, crucial for the correct electron transfer and finalisation of the catalytic event, is strongly influenced by the flexibility of the peptide linker connecting the different domains of the protein and can be modulated by modification of the length of this loop. These P450 3A4 chimeric enzymes, 3A4-BMR, 3A4-3GLY-BMR and 3A4-5GLY-BMR were engineered with an inter-domain loop containing no glycine residues, three glycine residues or five glycine residues respectively. Catalytic activity of these 3A4-BMR chimeras proved to be strongly dependent on the inter-domain flexibility with 3A4-5GLY-BMR variant being the most efficient in the biotransformation of both testosterone and erythromycin substrates [7,8]. The better performance in catalytic activity was found strictly related to the coupling efficiency of the system that was proportionally dependent on the loop length [7,8].

The investigation on direct electrochemistry of multi-domain redox enzymes is very important for the understanding of the electron transport across the different modules of the chimeric enzyme. For the NADPH-cytochrome P450 reductase (CPR)-P450 electrodes, it has been previously demonstrated that they closely mimic the natural catalytic system [10-14]. In majority of the cases,

the presence of CPR in the electrochemical setup can significantly improve electrochemically-driven catalytic performance of the protein [10-14]. This is particularly relevant in the case of our engineered 3A4-BMR chimeras for which the influence of the inter-domain flexibility on electron transfer efficiency was already demonstrated [7,8]. Electrochemical studies on P450 3A4 artificial redox systems engineered by genetic fusion of its haem domain with the reductase domain of different redox chains demonstrated that the regulation of the electron flow through the multi-domain enzyme can significantly improve both catalytic activity and coupling efficiency at the electrode surface [15]. Moreover, it has been reported that the different immobilisation technique used, both in terms of physical-chemical properties of the immobilising film and in terms of electrode surface, can affect redox properties and catalytic efficiency of immobilised P450 enzymes [16,17].

In this work, we study the direct electrochemistry of 3A4-BMR fusion proteins on glassy carbon electrodes with the aim of investigating the influence on redox properties of the protein of the length of the inter-domain loop. In order to highlight the effect of the flexibility of the enzyme environment on both redox features and electrocatalysis, 3A4-BMR is immobilised using co-crosslinking technique with glutaraldehyde as bi-functional linking agent and bovine serum albumin (BSA) as coadjutant inert protein. As previously reported, BSA-glutaraldehyde co-crosslinking gel shows an honeycomb-like structure characterized by a high degree of porosity [18]. This immobilisation technique offers the possibility of obtaining different degrees of flexibility by modulating the glutaraldehyde amount in the composition of the crosslinking gel. In particular, glutaraldehyde concentration is directly related to co-crosslinking gel rigidity [19]. For these reasons, 3A4-BMR chimeras are immobilised on glassy carbon electrodes using 14 % , 7 % and 4 % glutaraldehyde co-crosslinking gel and redox properties of the multi-domain enzymes are studied by cyclic voltammetry in their ligand free form or after binding with testosterone substrate or ketoconazole inhibitor. Electrocatalysis is also performed in the presence of the substrates

testosterone and tamoxifen. Results are related to those obtained in solution by comparison with previously reported data in the case of testosterone [7] and with here presented kinetics issues in the case of tamoxifen. The chimeras are also studied by H/D exchange kinetics measured by Attenuated Total Reflectance-Fourier Transform Infrared (ATR-FTIR) spectroscopy.

FTIR offers the possibility to investigate secondary structure elements in relation to protein folding, while H/D exchange provides important information on structural dynamics and inter-domain flexibility [20,21].

## 2. Material and methods

### 2.1. Chemicals

Analytical grade chemical products (Sigma Aldrich) were used with no further purification in analytical grade after dissolution in ultrapure deionised water or in the appropriate organic solvent immediately before use.

### 2.2. 3A4-BMR fusion proteins expression and purification

3A4-BMR fusion proteins were previously engineered as reported by Degregorio *et al.* in 2017 [7]. Heterologous expression in competent *E. coli* DH5α cells and purification using two step ion exchange chromatography was performed using the procedure described by Dodhia *et al.* in 2006 [6].

### 2.3. ATR-FTIR experiments

FTIR experiments were performed at room temperature on Bruker Model Tensor 27 FT-IR spectrophotometer (Bruker Instruments, USA) using ATR tool (Harrick Scientific Products, USA) with 10 kHz as scan velocity and 4 $cm^{-1}$ as resolution by depositing a thin protein film (30 µL, 50 µM) directly on ATR reflection crystal. Spectra were collected between 4000 and 800 $cm^{-1}$ wavenumbers. During acquisition, the spectrophotometer sample chamber was continuously purged with nitrogen.

H/D exchange experiments were performed by FTIR using the procedure described by Di Nardo *et al.* in 2013 [22] with modification. In particular, purging nitrogen was enriched with $D_2O$ by bubbling into a bottle containing 200 mL of $D_2O$. Spectra were collected at 2 minutes intervals for 46 minutes. For each time point 60 scans were collected and averaged. Spectra were collected in triplicate and averaged for each time point. The H/D exchange was monitored by following the changes in the Amide II band by analysing averaged spectra corrected by buffer subtraction and normalized by Amide I band. H/D exchange kinetics were studied by fitting relative absorbance as function of time using SigmaPlot software.

### 2.4. 3A4-BMR Electrode preparation

3A4-BMR fusion proteins were immobilised on 3 mm diameter glassy carbon working electrodes (BASi, USA) by co-crosslinking with glutaraldehyde and BSA using the procedure described by Castrignanò *et al.* in 2010 with modification [23]. In particular, three different composition of the co-crosslinking gel were used starting from ~50 μM 3A4-BMR protein solution:

1) 14 % glutaraldehyde gel: 6 μL of 3A4-BMR protein solution + 6 μL of 2 mM BSA solution + 2 μL of 20 % glutaraldehyde solution,
2) 7 % glutaraldehyde gel: 6 μL of 3A4-BMR protein solution + 7 μL of 2 mM BSA solution + 1 μL of 20 % glutaraldehyde solution;
3) 4 % glutaraldehyde gel: 6 μL of 3A4-BMR protein solution + 7.5 μL of 2 mM BSA solution + 0.5 μL of 20 % glutaraldehyde solution.

The three glutaraldehyde gel concentration is the percent dilution from the 20% glutaraldehyde stock solution. In all cases, the final volume of the co-crosslinking solution was 14 μL. After the addition of glutaraldehyde, the co-crosslinking solution was rapidly and gently mixed and 2 μL were immediately pipetted on the glassy carbon electrode surface previously cleaned by polishing on alumina and sonication in ultra-pure deionized water. After O/N air drying at 4 °C, the electrode was stirred for 1 min in electrolysis phosphate buffer to enable the soaking of the gel.

For the experiments performed in the presence of testosterone and ketoconazole, co-crosslinking gel composition was enriched with the correspondent drug by addition to the BSA solution in order to obtain a final concentration in the gel of 200 μM for testosterone and 20 μM for ketoconazole.

### 2.5. Cyclic voltammetry and chronoamperometry experiments

All electrochemical experiments were performed at room temperature (25 °C) and in 50 mM phosphate buffer pH 7.4, with addition of 100 mM KCl as supporting electrolyte. An Autolab PGSTAT12 potentiostat (Ecochemie, The Netherlands) controlled by GPES3 software was used to perform both cyclic voltammetry and electrocatalysis experiments. Glassy carbon working electrode was opportunely connected to a conventional electrolysis cell, together with a platinum wire counter electrode and an Ag/AgCl (3 M NaCl) reference electrode (BASi, USA).

Direct electrochemistry investigation of 3A4-BMR fusion proteins immobilised by co-crosslinking was performed by cyclic voltammetry in anaerobiosis within a glovebox (Belle Technologies, U.K.). Cyclic voltammograms were recorded between 200 and -750 mV using different scan rate values depending on experimental purposes. Control experiments were performed on BSA-glutaraldehyde glassy carbon electrodes prepared using bare storage buffer instead of protein solution.

Electrocatalysis experiments on 3A4-BMR co-crosslinking electrodes were performed in the presence of both testosterone and tamoxifen substrates in saturating amount (200 μM) using chronoamperometry with an applied potential bias of -650 mV for 30 min. In order to allow substrate permeation into the enzymatic layer and minimize mass transport effect at the electrode surface, electrocatalysis experiments were performed by immobilising 3A4-BMR chimeras on rotating disk glassy carbon electrodes connected to a BASi RDE-2 rotator system (BASi, USA) set at 200 rpm rotation speed. Rotation speed value was chosen after preliminary study on its effect on the catalytic rate (data not shown). We found that 200 rpm is a good compromise between mass transport effect control and the limitation of the protein layer dissolution into the electrochemical

cell solution. Immediately after the chronoamperometry procedure, the electrocatalysis sample was analysed by HPLC in order to quantify the product amount, using the method described in the section 2.6.

### 2.6. Tamoxifen catalysis in solution

Tamoxifen N-demethylation activity of 3A4-BMR fusion proteins was characterized in solution using NADPH reducing equivalents. The enzymatic reaction was performed by incubating 1 μM enzyme for 5 minutes with tamoxifen using a concentration range between 5 and 200 μM. The reaction was then started by adding 500 μM NADPH. The reaction linearity was assessed over a 40 minutes time. After 30 minutes, the reaction was stopped by adding 10 μL/250 μL of 10 M HCl and by clarifying the solution by centrifugation at 14000 rpm for 5 minutes. The catalysis solution was then immediately analysed by HPLC for the product quantification, using the procedure described in the section 2.7.

### 2.7. High Performance Liquid Chromatography (HPLC)

The identification and quantification of product formed by 3A4-BMR fusion proteins both by electrocatalysis and by catalysis in solution, was performed using HPLC coupled with a diode array UV detector (Agilent-1200, Agilent technologies, USA) equipped with a 4.6 x 250 mm, 5 μm C18 column. Testosterone and 6β-hydroxytestosterone were separated using a gradient elution programmed as follows: isocratic elution of 20 % acetonitrile and 80 % water, 0-2 min; linear gradient elution from 20 % to 90 % acetonitrile and from 80 % to 10 % water, 2-20 min; linear gradient elution from 90 % to 20 % acetonitrile and from 10 % to 80 % water, 20-22 min; isocratic elution of 20 % acetonitrile and 80 % water, 22 min-end of the run. The flow rate was set at 1 mL/min and detection wavelength was 244 nm. Retention times were 9.2 min and 13.1 min for 6β-testosterone and testosterone, respectively. Tamoxifen and N-desmethyltamoxifen were separated using a gradient programmed as follows: isocratic elution of 30 % of 1 % triethylamine and 70% methanol, 0-2 min; linear gradient elution from 30 % to 15 % of 1 % triethylamine and from 70 %

to 85 % methanol, 2-3.5 min; isocratic elution of 15 % of 1 % triethylamine and 85 % methanol, 3.5-15 min; linear gradient elution from 15 % to 30 % of 1 % triethylamine and from 85 % to 70% methanol, 15-20 min. The flow rate was set at 1 mL/min and detection wavelength was 278 nm. Retention times were 11.2 min and 13.0 min for N-desmethyltamoxifen and tamoxifen, respectively.

### 2.8. Statistical analysis

All collected data were recorded at least in triplicate and expressed as mean ± standard deviation. The comparison of the results obtained was performed by one way ANOVA and two way ANOVA followed by Student-Newman-Keuls post hoc test using SigmaPlot software.

## 3. Results and discussion

### 3.1. H/D exchange kinetics by FTIR

The rate of H/D exchange is a very useful tool for the investigation of protein dynamics and flexibility and is particularly interesting to probe the structural plasticity of different linked domains [24,25]. Infrared spectral changes observed upon H/D exchange in protein samples are mainly related to Amide bands stretches. In particular, Amide I band (~1650 $cm^{-1}$) is only slightly affected by proton to deuterium exchange since it is primarily due to the stretching of the peptide C = O group [26]. Amide II band (~1550 $cm^{-1}$) is highly sensitive to environment deuteration degree since it is mainly due to the combination of in plane N – H bending and C – N stretching of the peptide bond [26]. Since during H/D exchange N – H bonds are converted into N – D bonds, Amide II band absorption related to N – H bending decreases proportionally with the fraction of H/D exchanged protein protons [25]. Figure 1 shows FTIR spectra of both P450 3A4 native protein and 3A4-BMR chimeras collected before and at the end of H/D exchange experiments. As can be seen, the main spectral change observed upon deuteration is the decrease of Amide II signal absorbance.

In order to investigate H/D exchange kinetics, the rate of protein deuteration was estimated by calculating the fraction of unexchanged amide protons (F) for each time point as a ratio of Amide II

band absorption to the Amide II absorption of the protein in $H_2O$ (time 0). The kinetic parameters of H/D exchange were calculated by plotting the decay of unexchanged protons fraction over time and by fitting it with single or double exponential functions. The plot of unexchanged protons fraction versus time for both P450 3A4 and 3A4-BMR fusion proteins are reported in the Figure 2. As can be seen, in all cases the H/D exchange kinetics can be resolved into three populations of protons with different deuteration rates [24]. A first population is exchanged in the first 10-12 minutes and represents the more exposed protons. The rate of deuteration of these protons was estimated by fitting the first tract of the unexchanged protons fraction plot to a single exponential curve that resulted in a first rate constant ($k_1$). The remaining part of the curve was fitted to a double exponential function. This allows to distinguish a second population of less exposed protons, characterised by the rate constant $k_2$, and a third population of buried protons. These buried protons exchange at such slow rate and at $t \rightarrow \infty$ correspond to the fraction of non-exchangeable protons quantified by $F_0$. In keeping with published literature [20-22], we calculated the rate of deuteration of the first ($k_1$) and the second ($k_2$) population of protons since the third one is characterised by a very low rate of exchange. Kinetic parameters of H/D exchange for P450 3A4 and 3A4-BMR chimeras are summarized in the Table 1.

Table 1 shows that for P450 3A4 the first protons population is characterised by a slower kinetic compared to the second one. Compared to P450 3A4, $k_1$ and $k_2$ values of 3A4-BMR, 3A4-3GLY-BMR and 3A4-5GLY-BMR are influenced both by the presence of BMR and the three different loops. However, since the BMR domain is constant among these last three constructs, differences among them in terms of $k_1$ and $k_2$ can be ascribed to the effect of the loop. Statistical analysis of these samples shows that while there is no significant difference in the $k_2$ values of the less exposed protons, there is a significantly higher $k_1$ value for the 3A4-5GLY-BMR chimera compared to the other two. We interpret this result in terms of higher flexibility of the 5GLY loop that increases the exposure, hence exchange, of the protons at the interface of the two domains. Nevertheless, the

fraction of non-exchangeable protons ($F_0$) estimated shows significant differences ascribable to the different flexibility of the various constructs. In particular, this value is statistically lower for P450 3A4 compared to 3A4-BMR chimeras. Moreover, among 3A4-BMR fusion proteins $F_0$ value seem to be affected by the length of the loop connecting the two domains. In fact, the fraction of protons that cannot be exchanged in these experimental conditions has been found inversely proportional to the length of the peptide loop in 3A4-BMR, showing that the accessibility to H/D exchange is statistically correlated to inter-domain flexibility. A schematic summary of H/D exchange results obtained by ATR-FTIR on 3A4-BMR chimeric enzymes is shown in the Scheme 1. In the chimeras with the shorter linker (0 and 3 GLY), the BMR domain forms more contacts with the P450 domain and thus fewer protons are exchangeable (higher $F_0$). The construct with the longest linker (5GLY) allows more flexibility between BMR and P450 3A4 and therefore few contacts are formed.

**Cyclic voltammetry of 3A4-BMR chimeras on GC/BSA-glutaraldehyde electrodes**

Cyclic voltammetry experiments were performed on 3A4-BMR chimeras immobilised on GC electrodes by co-crosslinking with BSA and glutaraldehyde. As reported in the Fig. 3A, two different redox species were detected when scanning the potential between 200 and -750 mV, the first is clearly identifiable with a redox transition at a lower potential [a], the second [b] can only be identified by reduction peak since oxidation one is probably hidden in the low potential oxidation wave.

We assigned the [a] redox couple to the flavin reductase domain and the [b] reduction peak to haem catalytic domain of 3A4-BMR protein. Fig. 3B shows an overlay of 3A4-BMR cyclic voltammogram with a control electrode prepared using the same immobilisation procedure in the presence of buffer instead of protein solution, and P450 3A4/BSA-glutaraldehyde electrode. As can be seen, P450 3A4 protein shows a redox transition at a lower potential compared to 3A4-BMR chimera. The negative shift of P450 3A4 [b] redox peak potential observed upon linkage with BMR reductase domain was already observed on glassy carbon electrode and was attributed to the

presence of the flavin domain, since the removal of flavin cofactors from the BMR domain results in a restoration of the potential to a value closer to the one observed for P450 3A4 enzyme [10]. Similar results were observed by cyclic voltammetry on P450 3A4/CPR microsomal system in presence of CO [14]. The apparent surface coverage, expressing the amount of electroactive protein in the co-crosslinking gel, was determined by applying Faraday's law using [a] redox peak charge values resulting in 3 pmol $cm^{-2}$ (about 0.5 % of the total amount of protein loaded). No effect on the surface coverage was observed by changing the inter-domain loop length. No redox signals were observed, as expected, on control electrode.

To investigate the effect of the inter-domain flexibility on the electrochemical features of 3A4-BMR chimeras, the composition of the BSA/glutaraldehyde co-crosslinking gel was optimized by using different amount of glutharaldehyde in order to modulate the enzyme layer flexibility. It has been reported that the decrease in glutaraldehyde % in crosslinking gel composition leads to an increase of gel extensibility and to a decrease of the breaking stress [19], resulting in a modulation of gel flexibility. For the immobilisation of 3A4-BMR fusion proteins on glassy carbon electrode surface, BSA co-crosslinking gel was prepared using three different compositions containing 14 %, 7 % and 4 % glutaraldehyde. Following previously reported results [19], we assume that the lower is the glutaraldehyde amount the higher is the flexibility of the co-crosslinking gel immobilising 3A4-BMR protein.

Cyclic voltammetry study was carried out to evaluate the influence of the enzyme environment flexibility on the redox properties of 3A4-BMR fusion proteins. In particular, 3A4-BMR, 3A4-3GLY-BMR and 3A4-5GLY-BMR chimeras were immobilised on glassy carbon electrode using 14 %, 7 % and 4 % glutaraldehyde co-crosslinking gel with BSA, and the electrochemical parameters were estimated and compared as reported in the Table 2.

The flexibility of the enzyme environment seems to influence electron transfer properties of 3A4-BMR fusion proteins. In particular, [a] redox potential seems to be affected similarly for the three

chimeras and the increase in flexibility of the immobilising gel is correlated with a general tendency to a negative shift of $E_{1/2}$ value. For 3A4-BMR and 3A4-5GLY-BMR the negative shift of $E_{1/2}$-[a] has been found statistically significant only for the more flexible co-crosslinking gel (4 %) whereas for 3A4-3GLY-BMR a significant decrease of $E_{1/2}$ value for [a] redox couple was detected not only for 4 % but also for 7 % glutaraldehyde gel. The negative shift (~10 mV) observed for flavin domain potential in the more flexible environment (4 % glutaraldehyde co-crosslinking gel) is not strikingly significant from an electrochemical point of view. However, a decrease of reductase reducibility can impair the inter-domain electron transfer rate and lead to an improvement of the electrochemical tuning between the two domains. The gel flexibility seems not to influence the reduction peak potential of the [b] redox feature. Moreover, the gel flexibility seems also to significantly affect [a] peak-to-peak separation (ΔE) of the chimeric enzymes depending on the length of inter-domain loop. In fact, while for 3A4-BMR construct ΔE-[a] is statistically not influenced by glutaraldehyde %, for 3A4-3GLY-BMR and 3A4-5GLY-BMR a significant effect is observed leading to 57 % and 26 % decrease respectively. The decrease in ΔE can be interpreted as an improvement of electrochemical reversibility of [a] redox system.

Furthermore, some significant differences were found for 3A4-BMR chimeras immobilised using the same co-crosslinking gel composition as effect of the loop length. In particular, 3A4-3GLY-BMR $E_{1/2}$-[a] value resulted significantly lower compared to 0GLY in 7 % gel. When comparing [b] reduction peak potential values, again no significant differences were found. In addition, 3A4-3GLY-BMR ΔE-[a] value compared to 0GLY in 14 % gel, showing that 3GLY protein is the only one that shows irreversible redox system when using the more rigid gel composition.

In order to properly assign redox peaks observed by cyclic voltammetry on 3A4-BMR GC/BSA-glutaraldehyde electrodes, direct electrochemistry of ligand free immobilised enzyme was compared to ligand bound protein. In particular, 3A4-BMR fusion proteins were immobilised, using 4 % BSA/glutaraldehyde co-crosslinking gel, both in the presence of substrate, testosterone, and in

the presence of inhibitor, ketoconazole in saturating amounts. Cyclic voltammetry results of both testosterone and ketoconazole bound 3A5-BMR chimeric proteins are shown in the Figure 4 and summarized in the Table 3, in comparison with ligand free enzyme results. As can be seen, the presence of both testosterone and ketoconazole does not influence $E_{1/2}$ nor $\Delta E$ values for [a] redox species. A significant effect was detected on the redox potential of the [b] redox species depending on the nature of the ligand: a significant positive shift is detected upon binding of testosterone substrate whereas the presence of ketoconazole inhibitor leads to a statistical negative shift of the reduction potential value. The length of the glycine linker of the three 3A4-BMR construct seems not to significantly affect these potential shifts. The opposite effect on the [b] species reduction potential observed in the presence of testosterone and ketoconazole led us to assign [b] reduction peak to haem $Fe^{3+/2+}$ transition of the catalytic domain of 3A4-BMR chimeras. The positive shift of the haem redox potential observed upon substrate binding is well documented in literature as an essential step for the electron transfer from cytochrome P450 redox partners [27-29]. The negative potential shift observed upon binding of ketoconazole is also typically observed for the type II ligands and is related to the direct binding of the molecule to the haem by a nitrogen atom [30]. Consequently, we assigned [a] redox couple to FMN/FAD reductase domain. Similarly to our results on 3A4-BMR chimeras, direct electrochemistry experiments on immobilised cytochrome P450 BM3 previously reported about the cyclic voltammetry detection of two different redox systems [16]. Authors assigned the two redox transitions, centred at -388 mV and -250 mV, to cytochrome P450 BM3 reductase and haem domain respectively by investigating electron transfer properties of the two domains separately using the correspondent holoenzyme.

### 3.2. Tamoxifen catalysis by 3A4-BMR fusion proteins in solution

Catalytic activity of 3A4-BMR fusion proteins towards tamoxifen N-demethylation was assessed in solution in the presence of NADPH electron donor. Tamoxifen is a chemotherapeutic drug widely used in the treatment of breast cancer for its anti-estrogenic activity. Phase I metabolism of

tamoxifen, involving P450 enzymes, leads to its bioconversion into active metabolites meanly resulting from hydroxylation and demethylation reactions [31-33]. The major metabolite, N-desmethyltamoxifen, is predominantly produced by P450 3A4 activity and is characterised by anti-estrogenic activity similar to that of tamoxifen [34-36]. We previously demonstrated that 3A4-BMR catalytic activity towards the metabolism of P450 3A4 substrate drugs can be affected by the length of the loop connecting reductase and haem domain of the fusion proteins [7,8]. Tamoxifen N-demethylation activity of 3A4-BMR chimeras was studied in order to investigate the influence of the loop length on the metabolism of this drug. The results, reported in the Figure 5, show that, similarly to what previously observed for testosterone and erythromycin [7,8], 3A4-5GLY-BMR chimera is the most efficient also in the N-demethylation of tamoxifen. In particular, the calculated $V_{max}$ values were 0.0110 ± 0.0008 nmol $min^{-1}$, 0.0102 ± 0.0003 nmol $min^{-1}$ and 0.0195 ± 0.0009 nmol $min^{-1}$ for 3A4-BMR, 3A4-3GLY-BMR and 3A4-5GLY-BMR respectively. $V_{max}$ value for tamoxifen N-demethylation was statistically higher for 3A4-5GLY-BMR than for the other two fusion proteins ($P < 0.001$, one way ANOVA). The calculated $K_M$ values, 31.1 ± 7.6 μM, 22.1 ± 2.9 μM and 27.0 ± 4.7 μM respectively for 3A4-BMR, 3A4-3GLY-BMR and 3A4-5GLY-BMR were not found significantly different, confirming that the loop length does not affect substrate affinity for 3A4-BMR chimeras. These results are in agreement with previously published data on recombinant P450 3A4 enzymatic assay in human liver microsomes [34]. Differently from what observed for testosterone and erythromycin [7,8], no improvement of tamoxifen N-demethylation rate was observed when increasing 3A4-BMR loop length from 0 to 3 glycine residues. This might be due to intrinsic molecular characteristics of the drug and to its binding properties to P450 3A4 binding site. Probably, the accommodation of tamoxifen molecule into the binding pocket of 3A4-BMR haem domain, and the subsequent catalytic event, requires a higher degree of inter-domain flexibility than the one provided by the 3 glycine loop.

### 3.3. Electrocatalysis by 3A4-BMR fusion proteins on BSA-glutaraldehyde glassy carbon electrodes

The catalytic activity of 3A4-BMR fusion proteins was investigated on glassy carbon electrodes after immobilization by co-crosslinking with BSA and glutaraldehyde using the three different gel composition. In particular, 6β-hydroxylation of testosterone and N-demethylation of tamoxifen by 3A4-BMR were studied by using reducing equivalents directly delivered by the electrode surface. The same experiment was performed on immobilised P450 3A4 protein as a comparison. The results, expressed as rate of product formed, are reported in the Figure 6.

As for testosterone electrocatalysis (Figure 6-A), an effect of the loop length on the catalytic activity was observed, with a significant improvement of 6β-hydroxylation activity of 3A4-3GLY-BMR and 3A4-5GLY-BMR compared to 3A4-BMR. This effect seems to be combined to the flexibility of the immobilising environment since a significant improvement of 6β-hydroxytestosterone formation rate was detected when lowering the amount of glutaraldehyde in the gel and so when increasing gel flexibility. In the less flexible gel, 14 % glutaraldehyde, the catalytic performance of 3A4-BMR chimeras is statistically impaired even if the effect of the loop length is still observable. Moreover, the testosterone electrocatalysis by immobilised P450 3A4 was significantly slower than 3A4-BMR chimeras with no effect of gel flexibility on P450 3A4 catalytic activity. These results confirm our previously published data on the effect of the length of inter-domain peptide linker on testosterone metabolism by 3A4-BMR [7,8]. We also demonstrated that the influence on testosterone 6β-hydroxylation activity of the inter-domain flexibility can be further modulated by controlling the flexibility of enzyme environment on the electrode surface.

Similar results were observed for tamoxifen electrocatalysis by immobilised 3A4-BMR fusion proteins (Figure 6-B). No statistical differences were detected in tamoxifen N-demethylation activity between the three 3A4-BMR fusion proteins in either 14% or 7% glutaraldehyde co-

crosslinking gel (black and grey bars). However, the activity was significantly improved with the increased linker length among the three fusion proteins in the most flexible 4% gel (comparing the white bars). The tamoxifen N-demethylation activity is not as sensitive as testosterone 6β-hydroxylation to the length of linker and the glutaraldehyde co-crosslinking gel flexibility. This is likely owing to the difference between these two substrates. Although P450 3A4 has a large flexible substrate binding pocket, the binding of a bulky compound does involve in a significant open-and-close motion of the enzyme. Possibly, accommodation of the branched compound as tamoxifen would need more gyration of protein than it would for a rather compact compound as testosterone. The shorter linker and the more rigid gel environment might hinder the motions of the protein that are necessary for the substrate binding. Therefore, only with the most flexible environment (4% gel) and longer linker length does the electrocatalysis show the efficiency.

P450 3A4 results for electrochemically driven tamoxifen bioconversion confirm that, in absence of the reductase domain, a lower product formation rate is obtained compared to 3A4-BMR chimeras, similarly to what observed in the presence of testosterone. Furthermore, also in the presence of tamoxifen, no effect on enzyme turnover was observed due to the modulation of enzyme environment flexibility. In absence of reductase domain, electrons are delivered to P450 3A4 catalytic centre directly from the electrode surface. The lack of effect on P450 3A4 turnover rate of environmental flexibility seems to confirm that flexibility modulation can affect inter-domain inter-connectivity, and consequently electron transfer among the different domains, rather than substrate accessibility to enzyme.

## 4. Conclusions

The regulation of the electron flow through the different modules in self-sufficient enzymes is a crucial issue in the development of artificial multi-domain systems suitable for bio-technological purposes. We previously developed and characterised a P450 3A4 chimeric enzyme by genetically

fusing haem domain of this protein to cytochrome P450 BM3 reductase domain, BMR. Our previously reported findings [7,8] demonstrated that both coupling and catalytic efficiency can be influenced by the modulation of the length of the peptide loop connecting catalytic and reductase domain of the chimera showing that the inter-domain flexibility is a crucial issue in determining the activity of the self-sufficient enzyme.

Here we performed a further investigation on 3A4-BMR chimeras dynamics and flexibility by studying H/D exchange kinetics by FTIR. Our results confirmed the effect on inter-domain flexibility of the different loops showing that when increasing the loop length an increase in the rate of exchange of the more exposed protons is observed together with an increase of the overall H/D exchangeability of the protein multi-domain system. These results are in agreement with our previously published data on the capability of 3A4-BMR chimeras to use NADPH electrons to reduce cytochrome *c* that is strictly related to cytochrome *c* ability to interact with the BMR domain [7]. In that case, the rate of cytochrome c reduction was higher for 5GLY construct characterized by the higher flexibility.

Direct electrochemistry of 3A4-BMR chimeras was studied on glassy carbon electrodes by immobilising the enzyme in co-crosslinking gel of BSA and glutaraldehyde. The immobilising gel flexibility was modulated by changing the amount of glutaraldehyde and the effect on redox properties and electrocatalysis efficiency was investigated. Cyclic voltammetry experiments on immobilised 3A4-BMR fusion proteins allowed the detection of two redox transitions at different potential that were addressed to flavin and haem domains of the protein ([a] and [b], respectively).

The flexibility of the enzyme immobilising system showed to affect [a] redox properties in 3A4-BMR chimeras since the increase in flexibility of the co-crosslinking gel corresponds to a decrease of the reduction potential expressed as midpoint potential. Also [a] redox system reversibility, expressed as ΔE, seems to be differently affected by the gel flexibility depending on the length of

the peptide loop with 3A4-3GLY-BMR and 3A4-5GLY-BMR showing a significant decrease to 57 % and 26 % respectively.

The effect of the loop length on 3A4-BMR catalytic activity was confirmed by electrocatalysis of testosterone and tamoxifen substrates with 3A4-5GLY-BMR being the most efficient in both cases. Moreover, the increase in flexibility of immobilising gel seems also to improve the efficiency of electrocatalysis confirming that the interdomain dynamics is crucial for the enzyme activity and the finalization of the catalytic event.

Another interesting observation in this work is the suppression of the electrocatalysis activity of P450 3A4 comparing to the other three 3A4-BMR chimeras (Figure 6). This seems to indicate that the direct electron transfer to the 3A4 heme is not as efficient as that from a protein redox partner such as BMR even though the latter is also introduced artificially. The "natural" electron transfer pathway from FMN to heme is not efficiently mimicked by the electrode to heme electron transfer.

Taken together, our results confirm that in the development of artificial multi-enzyme systems a very important aspect is the design of the loop connecting the different domains since this can highly affect the inter-domain flexibility and rearrangement and influence the performance of the chimeric system also in terms of redox properties and electrocatalysis capabilities. Moreover, our data demonstrated the feasibility of this protein engineering approach for cytochromes P450 biotechnological application and the development of bio-electrochemical setup suitable for drug development and screening purposes.

**Acknowledgments:**

This work is dedicated in memory of Klaus Ruckpaul, whose contribution to the P450 field is invaluable and his wide views are still tangible through the P450 congress series initiated by him.

**Abbreviations:**

P450: cytochrome P450; BMR: *Bacillus megaterium* reductase; GC: glassy carbon; BSA: bovine serum albumin; HPLC: high performance liquid chromatography; FTIR: Fourier transform infrared spectroscopy; ATR: attenuated total reflectance.

**Acknowledgments and funding**

This research did not receive any specific grant from funding agencies in the public, commercial, or not-for-profit sectors.

**References**


[1] G. Gilardi, A. Fantuzzi, 19(11) (2001) 468-476.

[2] G. Gilardi, A. Fantuzzi, S.J. Sadeghi, Curr. Opin. Struct. Biol. 11(4) (2001) 491-499.

[3] A. Yarman, U. Wollenberger, F.W. Scheller, Electrochim. Acta 110 (2013) 63-72.

[4] E. Schneider, D.S. Clark, Biosens. Bioelectron. 39 (2013) 1-13.

[5] P. Nowak, M. Wozniakiewicz, P. Koscielniak, TrAC-Trend Anal. Chem. 59 (2014) 42-49.

[6] V.R. Dodhia, A. Fantuzzi, G. Gilardi, J. Biol. Inorg. Chem. 11 (2006) 903-916.

[7] D. Degregorio, S. D'Avino, S. Castrignanò, G. Di Nardo, S.J. Sadeghi, G. Catucci, G. Gilardi, Front. Pharmacol. 8 (2017) 121.

[8] S. Castrignanò, S. D'Avino, G. Di Nardo, G. Catucci, S.J. Sadeghi, G. Gilardi, Biochim. Biophys. Acta 1866(1) (2018) 116-125.

[9] X. Chen, J.L. Zaro, W.C. Shen, Adv. Drug Deliv. Rev. 65(10) (2013) 1357-69.

[10] N. Sultana, J.B. Schenkman, J.F. Rusling, J. Am. Chem. Soc. 127 (2005) 13460–13461.

[11] R. Nerimetla, C. Walgama, V. Singh, S.D. Hartson, S. Krishnan, ACS Catalysis 7 (2017) 3446-3453.

[12] D. Cui, L. Mi, X. Xu, J. Lu, J. Qian, S. Liu, Langmuir 30 (2014) 11833–11840.

[13] Y. Mie, M. Suzuki, Y. Komatsu, J. Am. Chem. Soc. 131 (2009) 6646–6647.

[14] S. Krishnan, D. Wasalathanthri, L. Zhao, J.B. Schenkman, J.F. Rusling, J. Am. Chem. Soc. 133 (2011) 1459–1465.

[15] V.R. Dodhia, C. Sassone, A. Fantuzzi, G. Di Nardo, S.J. Sadeghi, G. Gilardi, Electrochem. Comm. 10 (2008) 1744-1747.

[16] B.D. Fleming, Y. Tian, S.G. Bell, L.L. Wong, V. Urlacher, H.A. Hill, Eur. J. Biochem. 270(20) (2003) 4082-4088.

[17] A.K. Udit, N. Hindoyan, M.G. Hill, F.H. Arnold, H.B. Gray, Inorg. Chem. 44(12) (2005) 4109-4111.

[18] X. Ma, X. Sun, D. Hargrove, J. Chen, D. Song, Q. Dong, X. Lu, T.H. Fan, Y. Fu, Y. Lei, Sci. Rep. 6 (2016) 19370.

[19] A. Bigi, G. Cojazzi, S. Panzavolta, K. Rubini, N. Roveri, Biomaterials 22(8) (2001) 763-768.

[20] S.W. Englander, Protein folding intermediates and pathways studied by hydrogen exchange. Annu. Rev. Biophys. Biomol. Struct. 29 (2000) 213-238.

[21] J. Kong, S. Yu, Acta Biochim. Biophys. Sin. (Shanghai) 39(8) (2007) 549-559.

[22] G. Di Nardo, M. Breitner, S.J. Sadeghi, S. Castrignanò, G. Mei, A. Di Venere, E. Nicolai, P. Allegra, G. Gilardi, PLoS One. 8(12) (2013) e82118.

[23] S. Castrignanò, S.J. Sadeghi, G. Gilardi, Anal. Bioanal. Chem. 398(3) (2010) 1403-1409.

[24] J. Li, X. Cheng, J.C. Lee, Biochemistry 41(50) (2002) 14771-14778.

[25] S. Yu, F. Fan, S.C. Flores, F. Mei, X. Cheng, Biochemistry 45(51) (2006) 15318-15326.

[26] A. Barth, C.Q. Zscherp, Rev. Biophys. 35 (2002) 369-430.

[27] F.P. Guengerich, Biochemistry 22 (1983) 2811-2820.

[28] S.G. Sligar, D.L. Cinti, G.G. Gibson, J.B. Schenkman, Biochem. Biophys. Res. Commun. 90 (1979) 925-932.

[29] G. Di Nardo, S. Castrignanò, S.J. Sadeghi, R. Baravalle, G. Gilardi, Electrochem. Comm. 52 (2015) 25-28.

[30] I.F. Sevrioukova, T.L. Poulos, Dalton Trans. 42(9) (2013) 3116-3126.

[31] D.J. Boocock, K. Brown, A.H. Gibbs, E. Sanchez, K.W. Turteltaub, I.N. White, Carcinogenesis 23(11) (2002) 1897-1901.

[32] H.K. Crewe, L.M. Notley, R.M. Wunsch, M.S. Lennard, E.M. Gillam, Drug Metab. Dispos. 30(8) (2002) 869-874.

[33] K. Kiyotani, T. Mushiroda, Y. Nakamura, H. Zembutsu, Drug Metab. Pharmacokinet. 27(1) (2012) 122-131.

[34] J.K. Coller, N. Krebsfaenger, K. Klein, R. Wolbold, A. Nüssler, P. Neuhaus, U.M. Zanger, M. Eichelbaum, T.E. Mürdter, Br. J. Clin. Pharmacol. 57(1) (2004) 105-111.

**Table 1.** Fitted H/D exchange kinetics parameters.

| | $k_1$ ($min^{-1}$) | $k_2$ ($min^{-1}$) | $F_0$ |
|---|---|---|---|
| **P450 3A4** | 0.038 ± 0.003 | 0.094 ± 0.010 | 0.133 ± 0.014 |
| **3A4-BMR** | 0.028 ± 0.002** | 0.134 ± 0.015* | 0.372 ± 0.008*** |
| **3A4-3GLY-BMR** | 0.028 ± 0.001** | 0.156 ± 0.025* | 0.290 ± 0.010***,## |
| **3A4-5GLY-BMR** | 0.037 ± 0.004# | 0.149 ± 0.020* | 0.171 ± 0.011**,## |

* $P < 0.05$, ** $P < 0.01$, *** $P < 0.001$ compared to P450 3A4, # $P < 0.01$, ## $P < 0.001$ compared to 3A4-BMR; One-way ANOVA followed by Student-Newman-Keuls post hoc test. Data are expressed as mean ± standard deviation of three replicates.

**Table 2.** Comparison of electrochemical features of 3A4-BMR immobilised on GC electrodes by co-crosslinking with different glutaraldehyde % composition.

| | | BSA-glutaraldehyde 14% | BSA-glutaraldehyde 7% | BSA-glutaraldehyde 4% |
|---|---|---|---|---|
| **3A4-BMR** | **$E_{1/2}$-[a] / mV** | -369 ± 4 | -367 ± 6 | -380 ± 3* |
| | **ΔE-[a] / mV** | 63 ± 3 | 61 ± 7 | 57 ± 7 |
| | **$E_{red}$-[b] / mV** | -281 ± 2 | -281 ± 3 | -282 ± 2 |
| **3A4-3GLY-BMR** | **$E_{1/2}$-[a] / mV** | -366 ± 0 | -380 ± 2**$^{,\#}$ | -381 ± 2** |
| | **ΔE-[a] / mV** | 101 ± 5$^{\#\#}$ | 62 ± 10*** | 43 ± 7*** |
| | **$E_{red}$-[b] / mV** | -285 ± 1 | -282 ± 2 | -278 ± 4 |
| **3A4-5GLY-BMR** | **$E_{1/2}$-[a] / mV** | -370 ± 5 | -375 ± 0 | -380 ± 1* |
| | **ΔE-[a] / mV** | 69 ± 11 | 59 ± 8* | 51 ± 7** |
| | **$E_{red}$-[b] / mV** | -275 ± 3 | -273 ± 3 | -278 ± 4 |

* $P < 0.05$, ** $P < 0.01$, *** $P < 0.001$ compared to BSA-glutaraldehyde 14%, $^{\#}$ $P < 0.05$, $^{\#\#}$ $P < 0.001$ compared to 3A4-BMR; Two-way ANOVA followed by Student-Newman-Keuls post hoc test. Data are expressed as mean ± standard deviation of four replicates.

**Table 3.** Comparison of electrochemical features of 3A4-BMR immobilised on GC electrodes by 4% glutaraldehyde co-crosslinking gel in absence of ligand and in the presence of 200 μM testosterone substrate or 20 μM ketoconazole inhibitor.

| | E values / mV | No ligand | Testosterone | Ketoconazole |
|---|---|---|---|---|
| **3A4-BMR** | $E_{1/2}$-[a] | -380 ± 3 | -378 ± 2 | -377 ± 3 |
| | ΔE-[a] | 57 ± 7 | 55 ± 5 | 57 ± 2 |
| | $E_{red}$-[b] | -282 ± 2 | -257 ± 3** | -308 ± 2* |
| **3A4-3GLY-BMR** | $E_{1/2}$-[a] | -381 ± 2 | -379 ± 2 | -378 ± 2 |
| | ΔE-[a] | 43 ± 7 | 47 ± 4 | 52 ± 6 |
| | $E_{red}$-[b] | -278 ± 4 | -255 ± 1** | -304 ± 2** |
| **3A4-5GLY-BMR** | $E_{1/2}$-[a] | -380 ± 1 | -381 ± 1 | -381 ± 2 |
| | ΔE-[a] | 51 ± 7 | 49 ± 3 | 59 ± 5 |
| | $E_{red}$-[b] | -278 ± 4 | -257 ± 2** | -292 ± 3** |

* $P < 0.05$, ** $P < 0.001$ compared to ligand free enzyme; Two-way ANOVA followed by Student-Newman-Keuls post hoc test. Data are expressed as mean ± standard deviation of four replicates.

**Captions**

**Figure 1:** FTIR spectra of P450 3A4 (A) and 3A4-BMR (B) collected during H/D exchange experiment. Spectra are normalized by Amide I signal (~1650 $cm^{-1}$). Arrows highlight the decrease in absorbance of the Amide II band observed upon H/D exchange.

**Figure 2.** Normalized fractions of non-exchanged amide protons as function of $D_2O$ exposure time measured for P450 3A4 (A), 3A4-BMR (B), 3A4-3GLY-BMR (C) and 3A4-5GLY-BMR (D). Solid lines represent the best fit to one or two-exponential curves of the data points.

**Scheme 1.** Schematic representation of H/D exchange results on 3A4-BMR fusion proteins compared to P450 3A4 enzyme. In green are shown regions of interface where hydrogen can exchange with deuterium, in blue are buried regions where hydrogen cannot exchange.

**Figure 3.** A) Cyclic voltammetry features of 3A4-BMR on GC/BSA-glutaraldehyde 4% electrodes, arrows indicate flavin domain [a] and haem domain [b] redox transitions. B) Comparison of 3A4-BMR cyclic voltammogram (bold line) with control electrode (dashed line) and P450 3A4 electrode (grey line) with arrows indicating P450 3A4 [b] redox transitions. Scan rate 120 mV/s.

**Figure 4.** Comparison of cyclic voltammetry results obtained by immobilising 3A4-BMR (A), 3A4-3GLY-BMR (B) and 3A4-5GLY-BMR (C) on glassy carbon electrodes by co-crosslinking with BSA/glutaraldehyde 4 %. Ligand free enzyme results (thin line) are shown together with ligand bound enzyme results (bold line) in presence of testosterone substrate (1) or ketoconazole inhibitor (2). Scan rate 120 mV/s.

**Figure 5.** Michaelis-Menten kinetics for tamoxifen N-demethylation in solution by 3A4-BMR (circles), 3A4-3GLY-BMR (triangles) and 3A4-5GLY-BMR (squares). Data are expressed as mean ± standard deviation of three replicates.

**Figure 6.** Electrocatalysis results of 3A4-BMR fusion proteins on GC/BSA-glutaraldehyde electrodes in the presence of 200 μM testosterone (A) and 200 μM tamoxifen (B). 3A4-BMR enzyme was immobilised using 14 % (black bars), 7 % (grey bars) or 4 % (white bars) glutaraldehyde co-crosslinking gel. * $P < 0.001$ compared to BSA-glutharaldehyde 14%, $^{\#}$ $P < 0.05$, $^{\#\#}$ $P < 0.01$, $^{\#\#\#}$ $P < 0.001$ compared to 3A4-BMR; Two-way ANOVA followed by Student-Newman-Keuls post hoc test. Data are presented as product formation rate and expressed as mean ± standard deviation for three replicates.

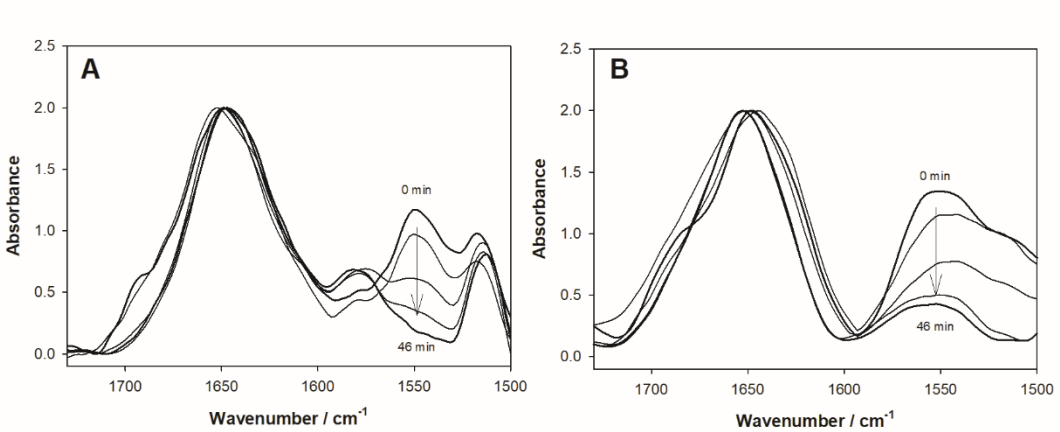


**Figure 1**

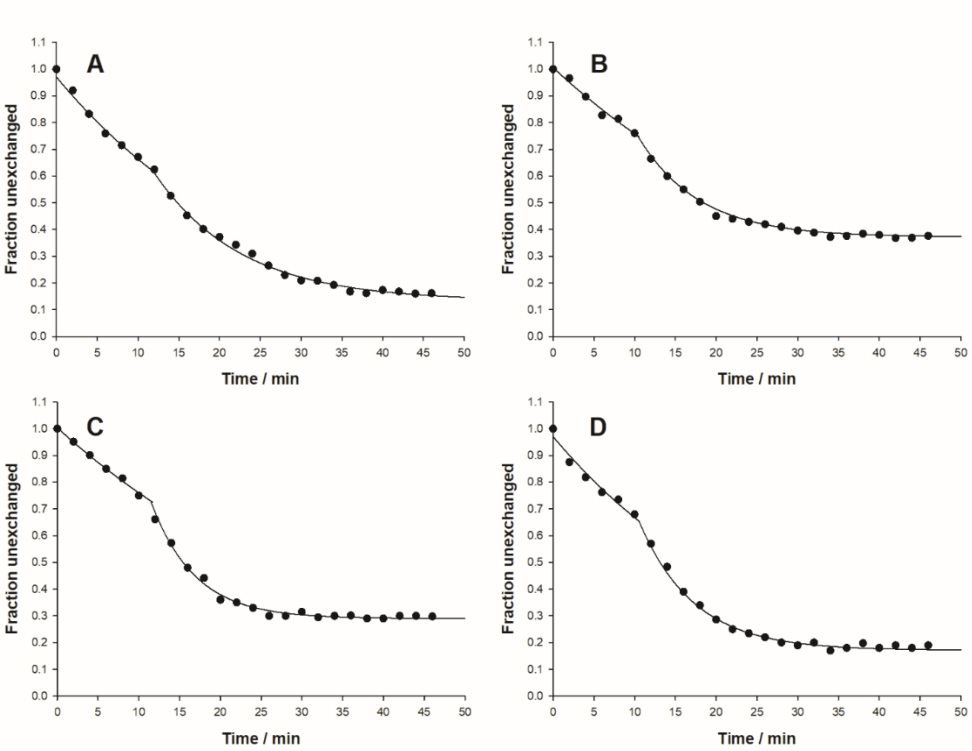


**Figure 2**

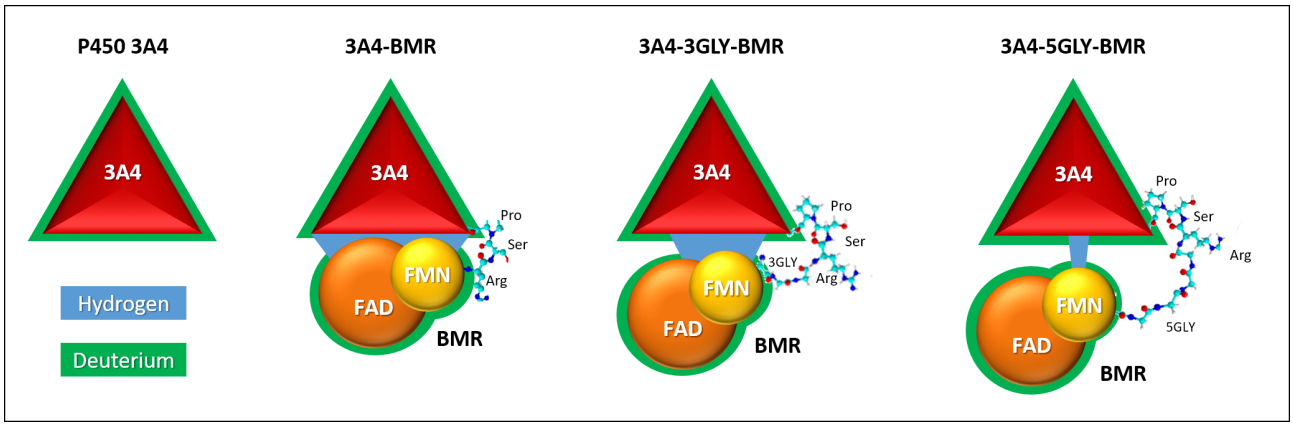


**Scheme 1**

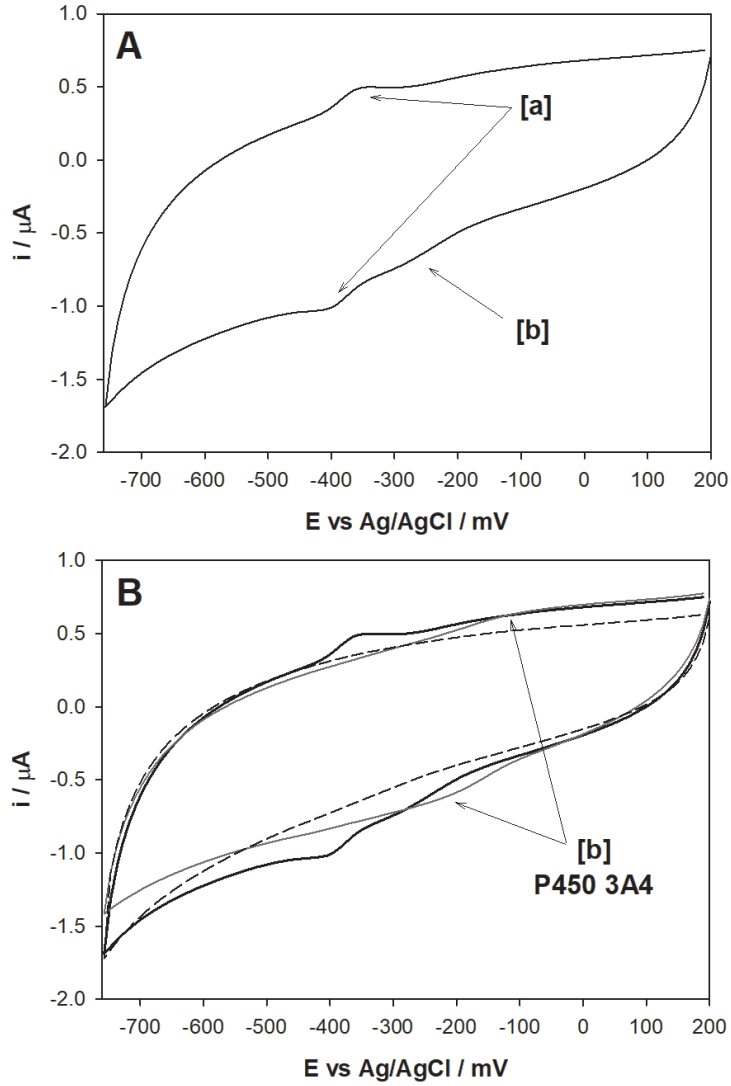


**Figure 3**

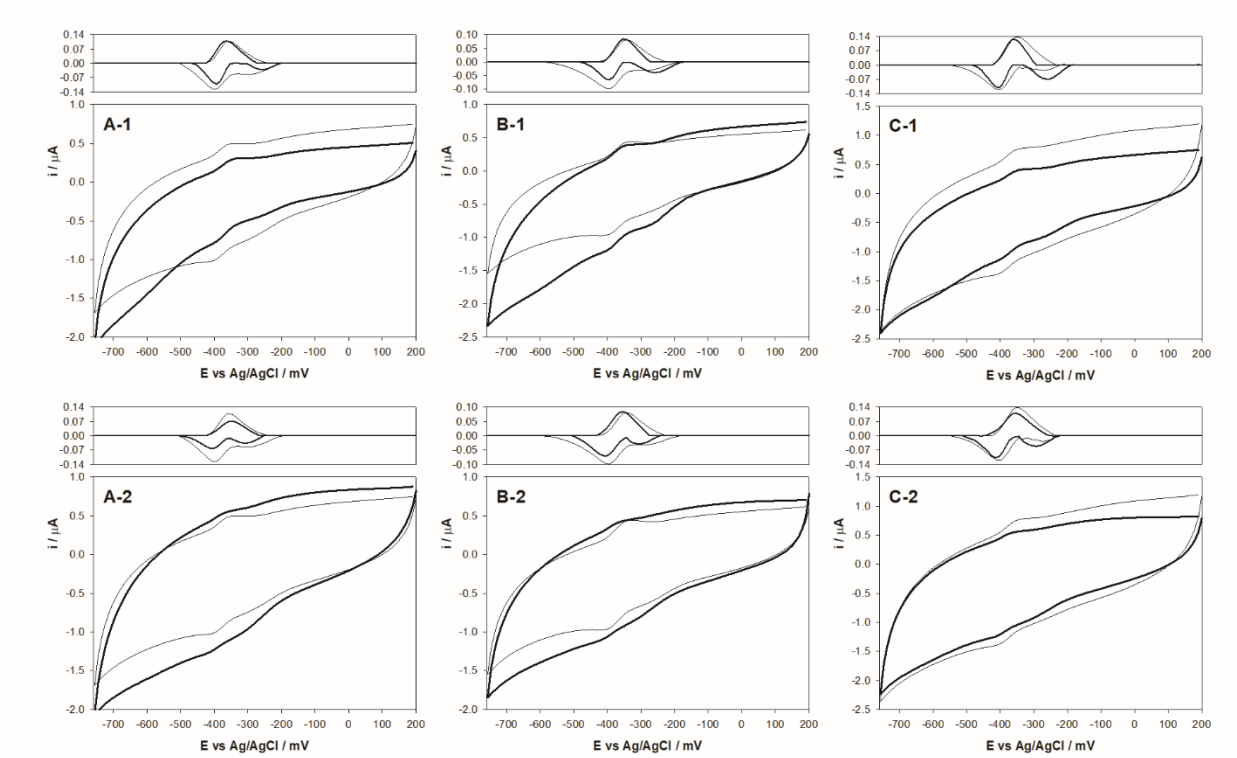


**Figure 4**

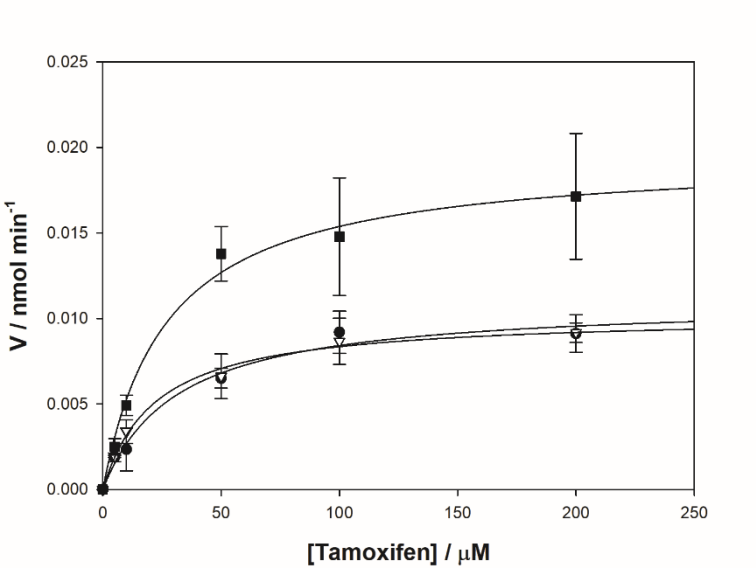


**Figure 5**

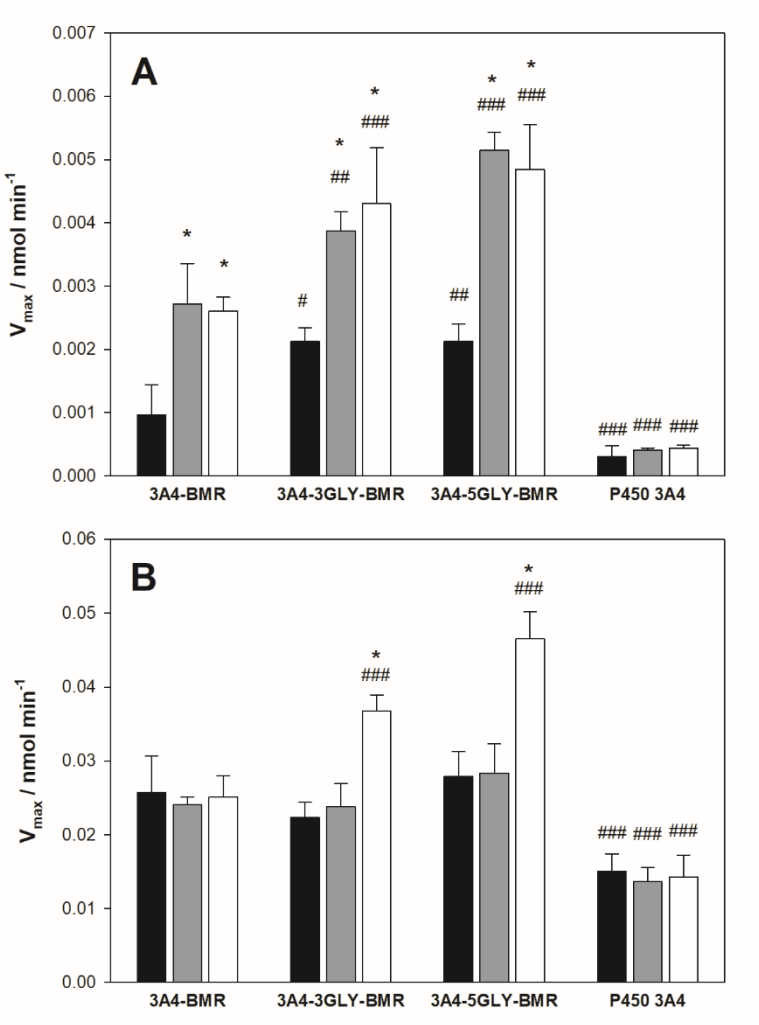


**Figure 6**